

High resolution infrared spectra of NGC 6440 and NGC 6441: * two massive Bulge Globular Clusters

L. Origlia¹, E. Valenti^{2,1,3}, R. M. Rich³

¹ *INAF-Osservatorio Astronomico di Bologna, Via Ranzani 1, I-40127 Bologna, Italy, e-mail livia.origlia@oabo.inaf.it*

² *ESO - European Southern Observatory, Vitacura, Santiago, Casilla 19001, Chile, e-mail evalenti@eso.org*

³ *Department of Physics and Astronomy, University of California at Los Angeles, Los Angeles, CA 90095-1562, e-mail rmr@astro.ucla.edu*

28 October 2018

ABSTRACT

Using the NIRSPEC spectrograph at Keck II, we have obtained infrared echelle spectra covering the 1.5 – 1.8 μm range for giant stars in the massive bulge globular clusters NGC 6440 and NGC 6441. We report the first high dispersion abundance for NGC 6440, $[\text{Fe}/\text{H}] = -0.56 \pm 0.02$ and we find $[\text{Fe}/\text{H}] = -0.50 \pm 0.02$ for the blue HB cluster NGC 6441. We measure an average α -enhancement of $\approx +0.3$ dex in both clusters, consistent with previous measurements of other metal rich bulge clusters, and favoring the scenario of a rapid bulge formation and chemical enrichment. We also measure very low $^{12}\text{C}/^{13}\text{C}$ isotopic ratios ($\approx 5 \pm 1$), suggesting that extra-mixing mechanisms are at work during evolution along the Red Giant Branch also in the high metallicity regime. We also measure Al abundances, finding average $[\text{Al}/\text{Fe}] = 0.45 \pm 0.02$ and $[\text{Al}/\text{Fe}] = 0.52 \pm 0.02$ in NGC 6440 and NGC 6441, respectively, and some Mg-Al anti-correlation in NGC 6441. We also measure radial velocities $v_r = -76 \pm 3$ km/s and $v_r = +14 \pm 3$ km/s and velocity dispersions $\sigma = 9 \pm 2$ km/s and $\sigma = 10 \pm 2$ km/s, in NGC 6440 and NGC 6441, respectively.

Key words: Galaxy: bulge, globular clusters: individual (NGC 6440 and NGC 6441) — stars: abundances, late-type — techniques: spectroscopic

1 INTRODUCTION

Over the past few years we have been undertaking a high-resolution spectroscopic survey of the Galactic bulge in the near-IR using NIRSPEC, a high throughput infrared (IR) echelle spectrograph at the Keck Observatory (McLean 1998). The near IR spectral range is well suited to measure the obscured stellar populations in the inner Galaxy. H-band (1.5–1.8 μm) spectra of bright giants in the bulge globular clusters and field population are ideal for detailed abundance analysis of Fe, C, O and other α -elements, using the approach of synthesizing the entire spectrum. The abundance distributions in the *cluster* and *field* populations are important in constraining the history and timescale of bulge formation and chemical enrichment (Rich 1990; McWilliam 1997; Matteucci, Romano & Molaro 1999r98).

We have used this method to derive abundances for

eight bulge globular clusters in the inner and outer bulge: the resulting abundances for NGC 6553 and Liller 1 are given in Origlia, Rich & Castro (2002), for Terzan 4 and Terzan 5 in Origlia & Rich (2004), for NGC 6342 and NGC 6528 in Origlia, Valenti & Rich (2005), and for NGC 6539 and UKS 1 in Origlia et al. (2005). We also measured detailed abundances of bulge giants in the Baade’s window (Rich & Origlia 2005) and in the inner field at $(l, b) = (0, -1)$ (Rich, Origlia & Valenti 2007).

We find α -enhancement at a level of a factor between 2 and 3 over the whole range of metallicity spanned by the bulge clusters in our survey, from $[\text{Fe}/\text{H}] \approx -1.6$ (cf. Terzan 4) up to $[\text{Fe}/\text{H}] \approx -0.2$ (cf. Terzan 5). Such an enhancement has been also found in the observed bulge fields, without any evidence of vertical abundance and abundance pattern gradients.

In this paper we present the high resolution IR spectra and the abundance analysis of bright giants in NGC 6440 and NGC 6441, two massive bulge globular clusters of the inner bulge, located at $(l, b) = (7.7, 3.8)$ and $(l, b) = (353.5, -5.0)$, respectively (Harris 1996).

During the 1990s, NGC 6440 has been photometrically observed in the optical (Ortolani, Barbuy & Bica

* Data presented herein were obtained at the W.M.Keck Observatory, which is operated as a scientific partnership among the California Institute of Technology, the University of California, and the National Aeronautics and Space Administration. The Observatory was made possible by the generous financial support of the W.M. Keck Foundation.

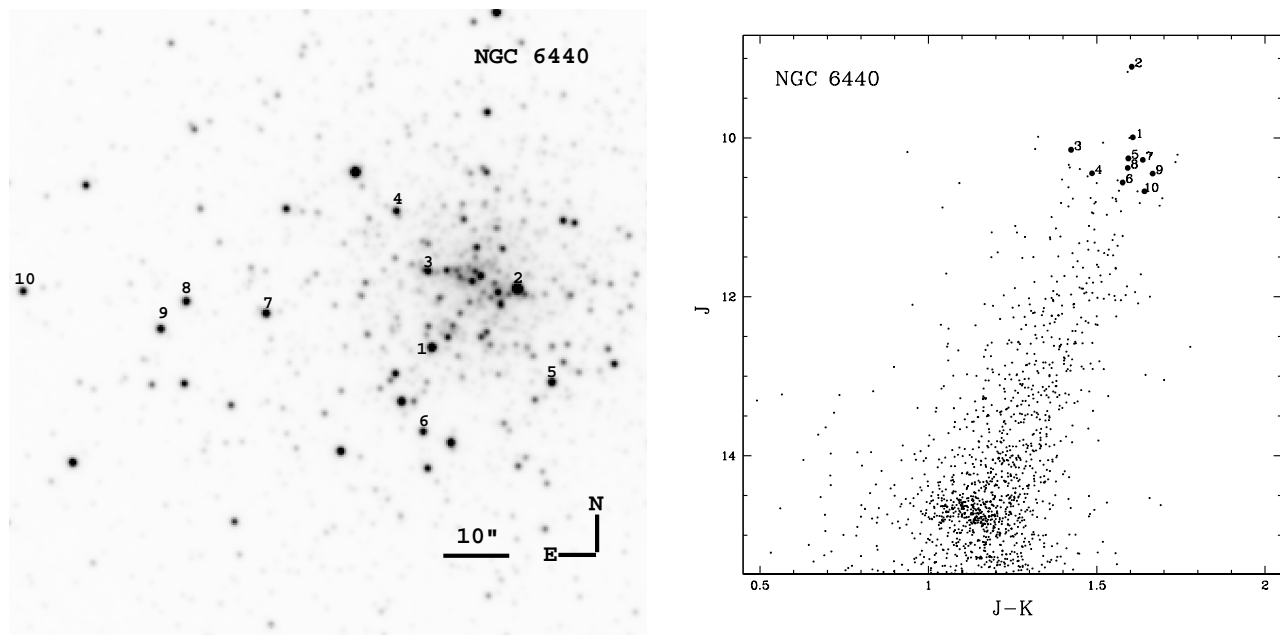


Figure 1. J band image of the core region (left panel) and the J,(J-K) color-magnitude diagram (right panel) of NGC 6440 (Valenti, Ferraro & Origlia 2004). The stars spectroscopically observed are numbered (cf. Table 1).

1994) and near IR (Kuchinski & Frogel 1995; Minniti 1995), suggesting an overall $[\text{Fe}/\text{H}]$ between 1/3 and half solar and $E(\text{B}-\text{V}) \approx 1.0 \pm 0.1$. Low resolution spectroscopy (Armandroff & Zinn 1988; Minniti 1995; Origlia et al. 1997; Frogel et al. 2001) provides very similar metallicities. More recently, Valenti, Ferraro & Origlia (2004) presented new near IR photometry, giving very similar $[\text{Fe}/\text{H}] = -0.49$ and slightly higher $E(\text{B}-\text{V}) = 1.15$, but in very good agreement with Schlegel, Finkbeiner & Davis (1998). No high spectral resolution measurements of this cluster exists so far.

NGC 6441 can be regarded as a twin cluster to NGC 6440, being also very massive and with an overall metallicity between 1/3 and half solar (Armandroff & Zinn 1988; Heitsch & Richtler 1999; Valenti, Ferraro & Origlia 2004), but with an anomalous blue horizontal branch (Rich et al. 1997) and RR Lyrae population (Clementini et al. 2005, and references therein) for its high metallicity. Given its lower $E(\text{B}-\text{V}) \approx 0.5 \pm 0.1$ extinction (see e.g. Gratton et al. 2006, for a review) compared to NGC 6440, this cluster has been also studied at high spectral resolution in the optical (Gratton et al. 2006, 2007), finding $[\text{Fe}/\text{H}] = -0.39$, $[\alpha/\text{Fe}]$ enhancement and Na-O anti-correlation.

Our observations and data reduction follow in Sect. 2. Sect. 3 presents our abundance analysis Sect. 4 the resulting chemical abundances and radial velocities. We discuss our findings in Sect. 5.

2 OBSERVATIONS AND DATA REDUCTION

Near infrared, high-resolution echelle spectra of bright giants in the core of the bulge globular clusters NGC 6440 and NGC 6441 have been acquired with the infrared spectrograph NIRSPEC (McLean 1998) mounted at the Nasmyth focus of the Keck II telescope. The high resolution

echelle mode, with a slit width of $0''.43$ (3 pixels) and a length of $12-24''$ and the standard NIRSPEC-5 setting, which covers most of the 1.5–1.8 micron H-band, have been selected. Typical exposure times (on source) are ≈ 8 minutes. NGC 6440 was observed on July 2003 and April 2007, while NGC 6441 on July and 2002 and May 2006. A total of 10 and 8 giants have been measured, respectively. Figs. 1, 2 show the IR image and the color-magnitude diagram (Valenti, Ferraro & Origlia 2004) of the central region of NGC 6440 and NGC 6441, respectively, with marked the giant stars spectroscopically observed. The selected stars are within a magnitude from the RGB Tip, that is sufficiently bright to give a good signal to noise in a relatively short integration time and sufficiently below the nominal RGB tip in order to minimize possible contamination by brighter AGB stars. Moreover, the selection of stars in the core region maximizes the membership probability, although a spectroscopic confirmation is always required. In NGC 6441 we also selected two stars (our # 7 and #8, right panel of Fig. 2) in common with Gratton et al. (2006) sample (their #7004050 and #7004434, respectively) for comparison, which lie in a more external field.

The raw two dimensional spectra were processed using the REDSPEC IDL-based package written at the UCLA IR Laboratory. Each order has been sky subtracted by using the pairs of spectra taken with the object nodded along the slit, and subsequently flat-field corrected. Wavelength calibration has been performed using arc lamps and a second order polynomial solution, while telluric features have been removed by dividing by the featureless spectrum of an O star. At the NIRSPEC resolution of $R=25,000$ several single roto-vibrational OH lines and CO bandheads can be measured to derive accurate oxygen and carbon abundances. Other metal abundances can be derived from the atomic lines of Fe I, Mg I, Si I, Ti I and Ca I. Abundance analysis

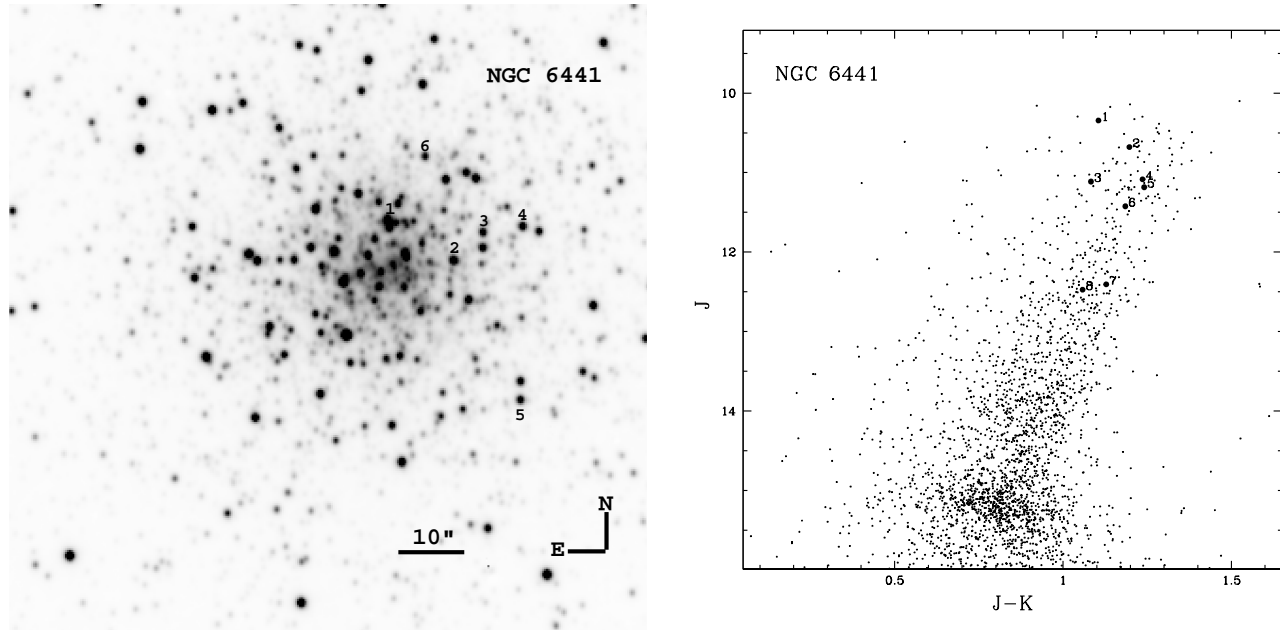


Figure 2. H band image of the core region (left panel) and the J,(J-K) color-magnitude diagram (right panel) of NGC 6441 (Valenti, Ferraro & Origlia 2004). The stars spectroscopically observed are numbered (cf. Table 2).

is performed by using full spectral synthesis techniques and equivalent width measurements of representative lines.

3 ABUNDANCE ANALYSIS

We compute suitable synthetic spectra of giant stars by varying the stellar parameters and the element abundances using an updated version (Origlia, Rich & Castro 2002) of the code described in Origlia, Moorwood & Oliva (1993). The main features of the code and overall spectral synthesis procedure have been widely discussed and tested in our previous papers and they will not be repeated here. We only mention that the code uses the LTE approximation and is based on the molecular blanketed model atmospheres of Johnson, Bernat & Krupp (1980) at temperatures ≤ 4000 K and the ATLAS9 models for temperatures above 4000 K. The reference solar abundances are from Grevesse & Sauval (1998).

Photometric estimates of the stellar parameters are initially used as input to produce a grid of model spectra, allowing the abundances and abundance patterns to vary over a large range and the stellar parameters around the photometric values. The model which better reproduces the overall observed spectrum and the equivalent widths of selected lines is chosen as the best fit model. We measure equivalent widths in the observed spectrum, in the best fit model and in four additional models which are, respectively, ± 0.1 and ± 0.2 dex away from the best-fitting, as a further cross-check of the inferred abundances and overall uncertainties listed in Tables 1,2.

Stellar parameter uncertainty of ± 200 K in temperature (T_{eff}), ± 0.5 dex in log-gravity ($\log g$) and ± 0.5 km s $^{-1}$ in microturbulence velocity (ξ), can introduce a further systematic ≤ 0.2 dex uncertainty in the absolute abundances. However, since the CO and OH molecular line profiles are

very sensitive to effective temperature, gravity, and micro-turbulence variations, they constrain better the values of these parameters, significantly reducing their initial range of variation and ensuring a good self-consistency of the overall spectral synthesis procedure (Origlia, Rich & Castro 2002; Origlia & Rich 2004).

Solutions with $\Delta T_{eff} = \pm 200$ K, $\Delta \log g = \pm 0.5$ dex and $\Delta \xi = \mp 0.5$ km s $^{-1}$ and corresponding ± 0.2 dex abundance variations from the best-fitting one are indeed less statistically significant (typically at $1 \leq \sigma \leq 3$ level only, Origlia & Rich (2004)). Moreover, since the stellar features under consideration show a similar trend with variation in the stellar parameters, although with different sensitivity, *relative* abundances are less dependent on stellar parameter assumptions, reducing the systematic uncertainty to < 0.1 dex.

4 RESULTS

By combining full spectral synthesis analysis with equivalent width measurements, we derive abundances of Fe, C, O and $^{12}\text{C}/^{13}\text{C}$ for the observed giants in NGC 6440 and NGC 6441. The abundances of additional α -elements, namely Ca, Si, Mg and Ti, are obtained by measuring a few major atomic lines. The $^{12}\text{C}/^{13}\text{C}$ isotopic ratio has been determined by using the ^{12}CO and ^{13}CO second overtone bandheads in the H band spectrum covered by our observations and a few isolated single roto-vibrational lines.

The near-IR spectra of cool stars also contain many CN molecular lines. However, at the NIRSPEC resolution most of these lines are faint and blended with the stronger CO, OH and atomic lines, making difficult to impossible a reliable estimate of the nitrogen abundance.

Stellar temperatures are both estimated from the (J -

Table 1. Photometric and photospheric parameters, heliocentric radial velocity, and chemical abundance patterns for the 10 giants observed in NGC 6440.

star	#1	#2	#3	#4	#5	#6	#7	#8	#9	#10
$(J - K)_0^a$	1.13	1.04	0.86	1.04	1.03	1.01	1.07	1.03	1.10	1.08
M_{bol}^a	-3.8	-4.8	-3.8	-3.3	-3.6	-3.3	-3.6	-3.5	-3.4	-3.2
T_{eff} [K]	3600	3600	3800	3600	3800	3800	3600	3600	3600	3600
$\log g$	0.5	0.5	0.5	0.5	0.5	0.5	0.5	0.5	0.5	0.5
v_r [km s $^{-1}$]	-80	-77	-86	-86	-52	-62	-67	-75	-71	-77
[Fe/H]	-0.53	-0.59	-0.65	-0.50	-0.55	-0.53	-0.55	-0.41	-0.56	-0.52
	± 0.07	± 0.08	± 0.10	± 0.09	± 0.10	± 0.10	± 0.09	± 0.07	± 0.09	± 0.09
[O/Fe]	0.32	0.27	0.33	0.30	0.45	0.43	0.33	0.25	0.31	0.34
	± 0.09	± 0.11	± 0.11	± 0.11	± 0.17	± 0.13	± 0.11	± 0.09	± 0.15	± 0.12
[Ca/Fe]	0.35	0.29	0.35	0.35	0.35	0.43	0.36	0.41	0.41	0.42
	± 0.11	± 0.12	± 0.15	± 0.13	± 0.13	± 0.13	± 0.13	± 0.11	± 0.13	± 0.13
[Si/Fe]	0.23	0.29	0.25	0.34	0.35	0.43	0.35	0.31	0.36	0.32
	± 0.23	± 0.23	± 0.19	± 0.24	± 0.21	± 0.21	± 0.24	± 0.24	± 0.24	± 0.24
[Mg/Fe]	0.31	0.28	0.30	0.33	0.35	0.40	0.35	0.33	0.34	0.33
	± 0.08	± 0.09	± 0.10	± 0.10	± 0.10	± 0.10	± 0.10	± 0.08	± 0.10	± 0.10
[Ti/Fe]	0.23	0.19	0.25	0.30	0.40	0.43	0.40	0.26	0.46	0.42
	± 0.15	± 0.15	± 0.19	± 0.16	± 0.15	± 0.15	± 0.16	± 0.13	± 0.16	± 0.16
[Al/Fe]	0.43	-	-	0.40	0.45	0.49	0.50	0.41	0.55	0.47
	± 0.13	-	-	± 0.14	± 0.15	± 0.15	± 0.14	± 0.14	± 0.14	± 0.14
[C/Fe]	-0.37	-0.41	-0.25	-0.30	-0.25	-0.27	-0.45	-0.29	-0.54	-0.48
	± 0.10	± 0.11	± 0.12	± 0.12	± 0.12	± 0.12	± 0.12	± 0.10	± 0.12	± 0.12
$^{12}\text{C}/^{13}\text{C}$	4.5	4.0	6.0	5.0	5.0	5.0	4.0	5.0	3.5	4.0
	± 1.2	± 1.0	± 1.6	± 1.3	± 1.3	± 1.3	± 1.0	± 1.3	± 0.9	± 1.0

^a J,K photometry, $E(B-V)=1.15$ and $(m-M)_0=14.58$ from Valenti, Ferraro & Origlia (2004).

Table 2. Photometric and photospheric parameters, heliocentric radial velocity, and chemical abundance patterns for the 8 giants observed in NGC 6441.

star	#1	#2	#3	#4	#5	#6	#7	#8
$(J - K)_0^a$	0.85	0.94	0.83	0.98	0.99	0.93	0.87	0.80
M_{bol}^a	-4.1	-3.8	-3.4	-3.3	-3.2	-3.0	-2.1	-2.0
T_{eff} [K]	4000	3800	4000	3800	3800	3800	4000	4000
$\log g$	1.0	0.5	1.0	1.0	1.0	1.0	1.0	1.0
v_r [km s $^{-1}$]	+33	+12	-1	+9	+13	+13	+20	+9
[Fe/H]	-0.55	-0.58	-0.49	-0.43	-0.45	-0.48	-0.56	-0.48
	± 0.10	± 0.08	± 0.16	± 0.08	± 0.08	± 0.08	± 0.08	± 0.08
[O/Fe]	0.28	0.35	0.26	0.23	0.17	0.23	0.29	0.33
	± 0.12	± 0.09	± 0.17	± 0.09	± 0.10	± 0.10	± 0.09	± 0.09
[Ca/Fe]	0.35	0.28	0.19	0.33	0.25	0.28	0.34	0.28
	± 0.16	± 0.13	± 0.20	± 0.15	± 0.15	± 0.15	± 0.13	± 0.13
[Si/Fe]	0.15	0.18	0.19	0.31	0.25	0.30	0.36	0.29
	± 0.19	± 0.20	± 0.22	± 0.21	± 0.21	± 0.21	± 0.18	± 0.18
[Mg/Fe]	0.09	0.29	0.25	0.29	0.24	0.30	0.36	0.34
	± 0.11	± 0.09	± 0.16	± 0.09	± 0.09	± 0.09	± 0.08	± 0.08
[Ti/Fe]	0.35	0.12	0.29	0.33	0.35	0.38	0.36	0.28
	± 0.21	± 0.17	± 0.24	± 0.14	± 0.14	± 0.14	± 0.18	± 0.18
[Al/Fe]	0.60	0.51	0.51	0.53	0.55	0.58	0.43	0.49
	± 0.16	± 0.14	± 0.20	± 0.14	± 0.15	± 0.14	± 0.14	± 0.14
[C/Fe]	-0.35	-0.30	-0.44	-0.67	-0.65	-0.62	-0.24	-0.32
	± 0.13	± 0.11	± 0.17	± 0.11	± 0.11	± 0.11	± 0.11	± 0.11
$^{12}\text{C}/^{13}\text{C}$	4.0	5.0	5.0	6.0	7.0	6.0	5.0	5.0
	± 1.0	± 1.3	± 1.3	± 1.6	± 1.8	± 1.6	± 1.3	± 1.3

^a J,K photometry, $E(B-V)=0.52$ and $(m-M)_0=15.65$ from Valenti, Ferraro & Origlia (2004).

K_0 colors and molecular lines, gravity from theoretical evolutionary tracks, according to the location of the stars on the Red Giant Branch (RGB), and adopting an average microturbulence velocity of 2.0 km/s (see also Origlia et al. 1997). Equivalent widths are computed by Gaussian fitting the line profiles, typical values being a few hundreds mÅ, and the overall uncertainty $\leq 10\%$. A table (see Table 3 with the measured equivalent widths of representative lines for the observed stars in NGC 6440 and NGC 6441 is available in electronic form.

In order to check further the statistical significance of our best-fitting solution, we compute synthetic spectra with $\Delta T_{\text{eff}} = \pm 200$ K, $\Delta \log g = \pm 0.5$ dex and $\Delta \xi = \mp 0.5$ km s $^{-1}$, and with corresponding simultaneous variations of ± 0.2 dex of the C and O abundances to reproduce the depth of the molecular features. We follow the strategy illustrated in Origlia & Rich (2004). As a figure of merit we adopt the difference between the model and the observed spectrum (hereafter δ). In order to quantify systematic discrepancies, this parameter is more powerful than the classical χ^2 test, which is instead equally sensitive to *random* and *systematic* scatters.

Since δ is expected to follow a Gaussian distribution, we compute $\bar{\delta}$ and the corresponding standard deviation for our best-fitting solution and the other models with the stellar parameter and abundance variations quoted above. We then extract 10,000 random subsamples from each *test model* (assuming a Gaussian distribution) and we compute the probability P that a random realization of the data-points around a *test model* display a $\bar{\delta}$ that is compatible with an ideal best-fitting model with a $\bar{\delta}=0$. $P \simeq 1$ indicates that the model is a good representation of the observed spectrum. The statistical tests are performed on portions of the spectra mainly containing the CO bandheads and the OH lines which are the most sensitive to the stellar parameters.

4.1 NGC 6440

In order to obtain a photometric estimate of the stellar temperatures and the bolometric magnitudes we use the near IR photometry by Valenti, Ferraro & Origlia (2004) and their $E(B-V)=1.15$ reddening and $(m-M)_0=14.58$ distance modulus. We also use the color-temperature transformations and bolometric corrections of Montegriffo et al. (1998), specifically calibrated for globular cluster giants. We constrain effective temperatures in the range 3500–4000 K, and we estimate bolometric magnitudes $M_{\text{bol}} \leq -3.2$ (see Table 1). The final adopted temperatures, obtained by best-fitting the CO and in particular the OH molecular bands which are especially temperature sensitive in cool giants, are also reported in Table 1.

Fig. 3 shows our synthetic best fit superimposed on the observed spectra of giant #4 in NGC 6440. From our overall spectral analysis we find average $[\text{Fe}/\text{H}] = -0.50 \pm 0.02$, $[\text{O}/\text{Fe}] = 0.33 \pm 0.02$ and $[\alpha/\text{Fe}] = 0.34 \pm 0.02$ (see Table 1). We also measure an average carbon depletion ($[\text{C}/\text{Fe}] = -0.36 \pm 0.03$ dex) and low $^{12}\text{C}/^{13}\text{C} \approx 4.6 \pm 0.7$ isotopic ratio.

Our best-fitting solutions have an average probability $P > 0.99$ to be statistically representative of the observed spectra. The other *test models* with different assumptions for the stellar parameters are only significant at $\approx 1\sigma$ (warmer stars with corresponding 0.2 dex higher abundances) and 3σ

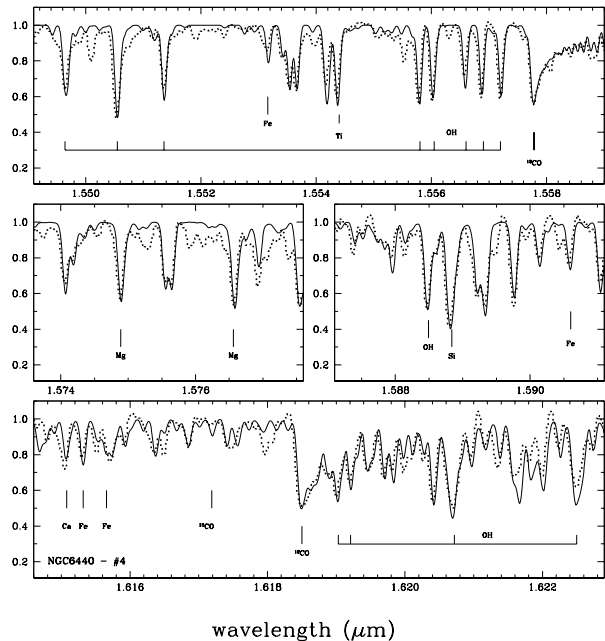


Figure 3. Selected portions of the observed echelle spectra (dotted lines) of star #4 in NGC 6440 with our best-fitting synthetic spectrum (solid line) superimposed. A few important molecular and atomic lines are marked.

(cooler stars with corresponding 0.2 dex lower abundances) level.

From the NIRSPEC spectra we also derived stellar heliocentric radial velocities (see Table 1), finding an average value $v_r = -74 \pm 4$ km/s with a dispersion $\sigma = 11 \pm 3$ km/s. By excluding star #5, which is the most discrepant, we find $v_r = -76 \pm 3$ km/s and $\sigma = 9 \pm 2$ km/s. These values are in good agreement with the one quoted in Harris (1996).

4.2 NGC 6441

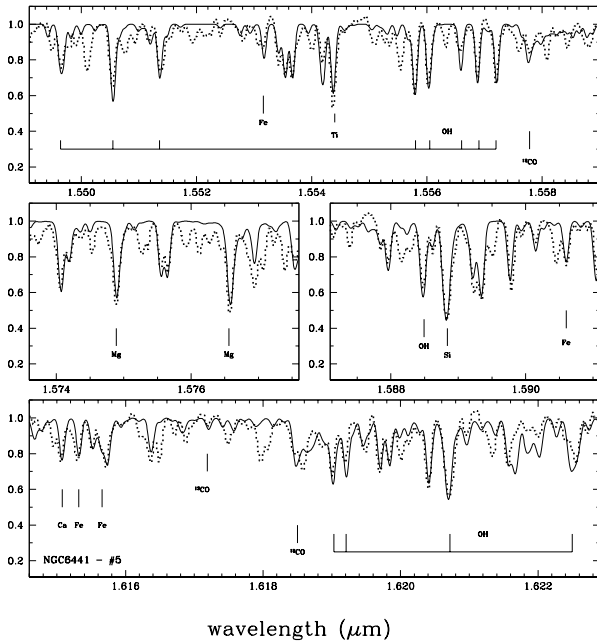
We use the near IR photometry of Valenti, Ferraro & Origlia (2004) and their $E(B-V)=0.52$ reddening and $(m-M)_0=15.65$ distance modulus. We find photometric temperatures in the 3800–4200 K range and bolometric magnitudes between -2.0 and -4.1 (see Table 2). The final adopted temperatures, obtained by best-fitting the CO and the OH molecular bands, are also reported in Table 2.

Fig. 4 shows our synthetic best-fitting superimposed on the observed spectra of giant #5 in NGC 6441. For this cluster our abundance analysis gives an average $[\text{Fe}/\text{H}] = -0.50 \pm 0.02$, $[\text{O}/\text{Fe}] = +0.27 \pm 0.02$ and an overall average $[\alpha/\text{Fe}] = 0.28 \pm 0.02$. We also measure an average carbon depletion ($[\text{C}/\text{Fe}] = -0.45 \pm 0.06$ dex) and a low $^{12}\text{C}/^{13}\text{C} \approx 5.4 \pm 0.9$.

Our iron abundance for stars #7 and #8 is only 0.10 dex lower and our average abundance 0.11 dex lower than in Gratton et al. (2006), so fully consistent within the errors. Our estimates for the other abundances are also similar (within ± 0.1 dex) with those quoted by Gratton et al. (2006). Only Ca, which is rather low in Gratton et al. (2006) compared to the other α -elements, is somewhat more dis-

Table 3. Log gf and equivalent widths (mÅ) of some representative lines for the observed stars in NGC 6440 and NGC 6441.

	Ca λ 1.61508	Fe λ 1.61532	Fe λ 1.55317	Mg λ 1.57658	Si λ 1.58884	OH λ 1.55688	OH λ 1.55721	Ti λ 1.55437	Al λ 1.67634
	Log gf								
	0.362	-0.821	-0.357	0.380	-0.030	-5.454	-5.454	-1.480	-0.55
	Equivalent widths in mÅ								
6440-1	220	209	170	395	502	325	331	352	357

**Figure 4.** Selected portions of the observed echelle spectra (dotted lines) of star #5 in NGC 6441 with our best-fitting synthetic spectrum (solid line) superimposed. A few important molecular and atomic lines are marked.

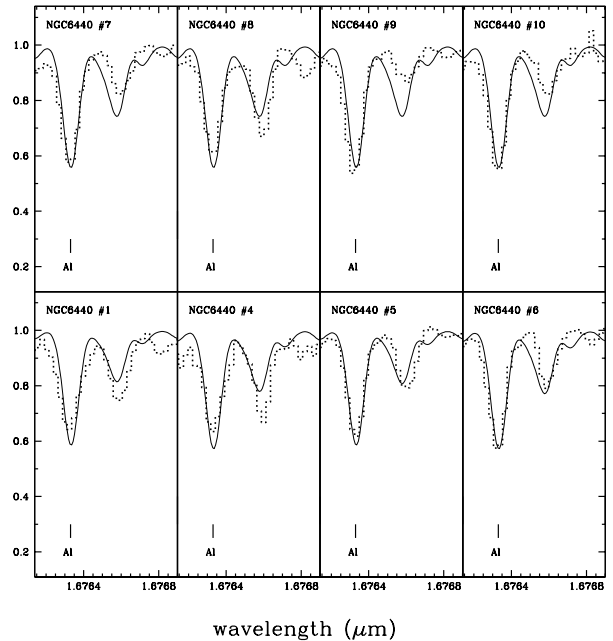
crepant (≈ 0.2 dex) but still barely consistent within the errors.

In order to further check the robustness of our best-fitting solutions, the same statistical test done for NGC 6440 has been repeated here. Our best-fitting solutions have an average probability $P > 0.99$ to be statistically representative of the observed spectra, while the other *test models* are only significant at $\geq 1 \sigma$ level.

By measuring the stellar radial velocities (see Table 2) we find an average $v_r = +13 \pm 3$ km/s with a dispersion $\sigma = 10 \pm 2$ km/s, somewhat lower, but still in reasonable agreement within the errors, with the values proposed by Gratton et al. (2007) based on a sample of stars three times larger, namely $v_r = +21$ km/s and $\sigma = 13$ km/s. Our radial velocity is in excellent agreement with the $v_r = +15$ km/s estimated by Dubath, Meylan & Mayor (1997).

4.3 Aluminum lines

The Al doublet at $\lambda\lambda 1.67506, 1.67634$ is at one side of the NIRSPEC-5 echellogram and easily measurable in stars with positive radial velocities as for the giants in

**Figure 5.** Observed spectra in the Al line region at $167 \mu\text{m}$, of the stars in NGC 6440 with our best-fitting synthetic spectrum (solid line) superimposed.

NGC 6441, while only the reddest line is barely measurable in the giants of NGC 6440. These lines have been proved to be reliable Al abundance indicators, having relatively high excitation potential and forming quite deeply in the stellar atmospheres, where the LTE regime still dominates, even in giants with low temperatures and gravities (see e.g. Baumüller & Gehren 1996). When available, the two lines of the doublet provide very similar Al abundances within the errors. However, since the $\lambda 1.67506$ line is very close to the edge of the echellogram, we only use it as a double check of the Al abundance obtained from the $\lambda 1.67634$.

Figs. 5, 6 show the observed spectra in the Al region with overimposed our best fit. The spectra of stars #2 and #3 in NGC 6440 were too noisy at $1.67 \mu\text{m}$ to be used for reliable Al abundance determinations.

We find average $[\text{Al}/\text{Fe}] = 0.45 \pm 0.02$ and $[\text{Al}/\text{Fe}] = 0.52 \pm 0.02$ in NGC 6440 and NGC 6441, respectively (see also Tables 1 and 2). Fig. 7 shows the plot of the $[\text{Mg}/\text{Fe}]$ vs $[\text{Al}/\text{Fe}]$ distribution for the two clusters. Although our samples are too small to draw firm conclusions, we find some evidence of an anti-correlation between the two abundance ratios in NGC 6441, with a Spearman rank correlation coefficient of -0.7 , corresponding to a probability of only $\approx 5\%$

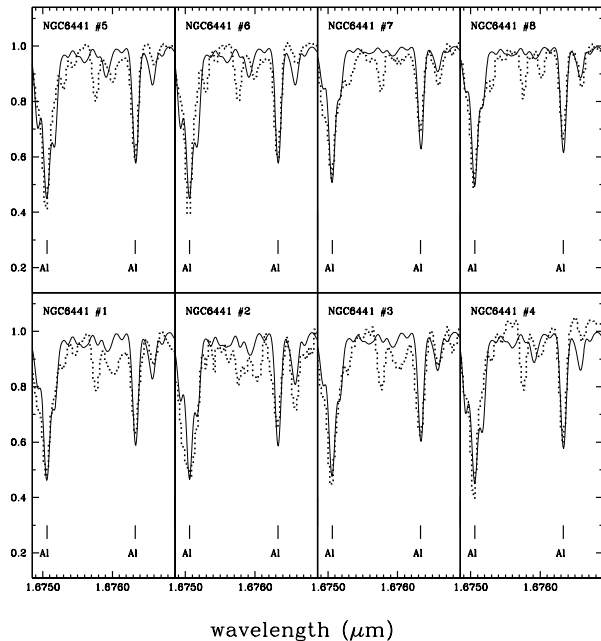


Figure 6. Observed spectra in the Al line region at $167 \mu\text{m}$, of the stars in NGC 6441 with our best-fitting synthetic spectrum (solid line) superimposed.

that the two variables be not correlated. Such an evidence is not presently detected in NGC 6440.

5 DISCUSSION AND CONCLUSIONS

Our high resolution spectroscopy in the near IR gives radial velocities well in agreement with previous studies, and typical ($|v_r| \leq \pm 100 \text{ km/s}$) of the bulge population. Also the inferred velocity dispersions are fully consistent with previous estimates and typical of massive globular clusters. Our iron abundances for NGC 6440 and NGC 6441 confirm the 1/3 solar abundance derived from photometric estimates, as obtained from the RGB morphology and luminosity in the optical as well as in the near IR.

The enhancement of the $[\alpha/\text{Fe}]$ abundance ratio, relative to the solar value, agrees well with other studies of clusters and bulge field. This reinforces the statement of an ab-origin enrichment of the interstellar medium by type SNII and an overall star formation process and chemical enrichment on a relatively short timescale.

The low $^{12}\text{C}/^{13}\text{C}$ isotopic abundance ratios measured in NGC 6440 and NGC 6441 are similar to those measured in other giant stars of the bulge (Origlia, Rich & Castro 2002; Shetrone 2003; Origlia & Rich 2004) and the other globular clusters of our survey, as well as in the halo clusters (Shetrone 1996; Gratton et al. 2000; Vanture, Wallerstein & Suntzeff 2002; Smith, Terndrup & Suntzeff 2002; Origlia et al. 2003), suggesting that additional mixing mechanisms due to *cool bottom processing* in the stellar interiors during the evolution along the RGB (see e.g. Charbonnel 1995; Denissenkov & Weiss 1996; Cavallo, Sweigart & Bell

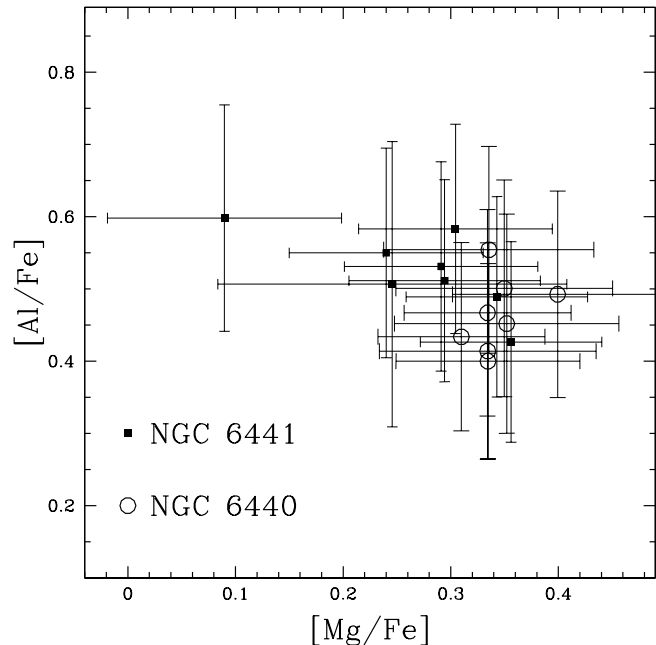


Figure 7. $[\text{Mg}/\text{Fe}]$ vs $[\text{Al}/\text{Fe}]$ abundance ratio distribution for the observed stars in NGC 6440 (open circles) and NGC 6441 (filled squares).

1998; Boothroyd & Sackmann 1999) occurs also at high metallicity.

O-Na and Mg-Al anti-correlations have been recently discovered in several massive globular cluster stars (see e.g. Sneden et al. 2004; Johnson et al. 2005; Gratton et al. 2007; Carretta 2006, and references therein). Recently, Gratton et al. (2006, 2007) also find evidence of such anti-correlations in NGC 6441. Such star-to-star abundance variations of O, Na, Al and Mg are currently interpreted as inhomogeneities in the proto-cluster gas, due to the pollution of a former generation of massive AGB stars. Indeed, the H-burning at high temperatures, as occurring in thermally pulsing AGB undergoing hot bottom burning (Ventura et al. 2001; Gratton et al. 2007), allows the O-N, Ne-Na and Mg-Al nucleosynthesis cycles (Langer, Hoffmann & Sneden 1993), although the latter requires higher temperatures than the previous ones, and produces less prominent abundance variations. Na-Al-rich and O-Mg poor globular cluster stars are thus expected to have formed within the kinematically cool ejecta of such a first generation of massive AGB stars (e.g. Cottrell & Da Costa 1981; Cohen, Briley & Stetson 2002).

ACKNOWLEDGMENTS

LO acknowledge the financial support by the Ministero dell'Istruzione, Università e Ricerca (MIUR).

RMR acknowledges support from grant number AST-0709479, from the National Science Foundation. The authors are grateful to the staff at the Keck Observatory and to Ian McLean and the NIRSPEC team. The authors wish to recognize and acknowledge the very significant cultural role and reverence that the summit of Mauna Kea has always had

within the indigenous Hawaiian community. We are most fortunate to have the opportunity to conduct observations from this mountain.

The authors acknowledge the anonymous Referee for his/her useful comments.

REFERENCES

- Armandroff, T. E., & Zinn, R. 1988, *AJ*, 96, 92
- Baumüller, D., & Gehren, T. 1996, *A&A*, 307, 961
- Boothroyd, A. I., & Sackmann, I. J. 1999, 1999, *ApJ*, 510, 232
- Carretta, E. 2006, *AJ*, 131, 1766
- Cavallo, R. M., Sweigart, A. V., & Bell, R. A. 1998, *ApJ*, 492, 575
- Charbonnel, C. 1995, *ApJ*, 453, L41
- Clementini, G., Gratton, R. G., Bragaglia, A., Ripepi, V., Fiorenzano, A. F. M., Held, E. V., & Carretta, E. 2005, *ApJ*, 630, 145
- Cohen, J. G., Briley, M. M., & Stetson, P. B. 2002, *AJ*, 123, 2525
- Cottrell, P. L., & Da Costa, G. S. 1981, *ApJ*, 245, 79
- Denissenkov, P. A., & Weiss, A. 1996, *A&A*, 308, 773
- Dubath, P., Meylan, G., & Mayor, M. 1997, *A&A*, 324, 505
- Ferraro, F.R., Montegriffo, P., Origlia, L. & Fusi Pecci, F. 2000, *AJ*, 119, 1282
- Frogel, J. A., Stephens, A., Ramirez, S., DePoy, D. L. 2001, *AJ*, 122, 1896
- Gratton, R., Sneden, C., Carretta, E., & Bragaglia, A. 2000, *A&A*, 354, 169
- Gratton, R. G., Sneden, C., & Carretta, E. 2004, *ARA&A*, 42, 385
- Gratton, R. G., Lucatello, S., Bragaglia, A., Carretta, E., Momay, Y., Pancino, E., & Valenti, E. 2006, *A&A*, 455, 271
- Gratton, R. G., et al. 2007, *A&A*, 464, 953
- Grevesse, N., & Sauval, A. J. 1998, *Space Science Reviews*, 85, 161
- Harris, W. E. 1996, *AJ*, 112, 1487
- Heitsch, F., & Richtler, T. 1999, *A&A*, 347, 455
- Johnson, H. R., Bernat, A. P., & Krupp, B. M. 1980, *ApJS*, 42, 501
- Johnson, C. I., Kraft, R. P., Pilachowski, C. A., Sneden, C., Ivans, I. I., Benman, G. 2005, *PASP*, 117, 1308
- Kuchinski, L. E., & Frogel, J. A. 1995, *AJ*, 110, 2844
- Langer, G. E., Hoffman, R., & Sneden, C. 2002, *PASP*, 105, 301
- Matteucci, F., Romano, D., & Molaro, P. 1999, *A&A*, 341, 458
- McLean, I. et al. 1998, *SPIE*, 3354, 566
- McWilliam, A. 1997, *ARA&A*, 35, 503
- Minniti, D., 1995, *A&A*, 303, 468
- Montegriffo, P., Ferraro, F.R., Fusi Pecci, F., & Origlia, L., 1995, *MNRAS*, 276, 739
- Origlia, L., Moorwood, A. F. M., & Oliva, E. 1993, *A&A*, 280, 536
- Origlia, L., Ferraro, F. R., Fusi Pecci, F., & Oliva, E. 1997, *A&A*, 321, 859
- Origlia, L., Rich, R. M., & Castro, S. 2002, *AJ*, 123, 1559
- Origlia, L., Ferraro, F. R., Bellazzini, M. & Pancino, E. 2003, *ApJ*, 591, 916
- Origlia, L., & Rich, R. M. 2004, *AJ*, 127, 3422
- Origlia, L., Valenti, E., & Rich, R. M. 2005, *MNRAS*, 356, 1276
- Origlia, L., Valenti, E., Rich, R. M., & Ferraro, F. R. 2005, *MNRAS*, 363, 897
- Ortolani, S. et al. 1994, *A&ASS*, 108, 653
- Rich, R. M. 1990, *ApJ*, 362, 604
- Rich, R. M., et al. 1997, *ApJ*, 484, 25
- Rich, R. M., & Origlia, L. 2005, *ApJ*, 634, 1293
- Rich, R. M., Origlia, L., & Valenti, E. 2007, *ApJ*, 665, 119
- Shetrone, M. d. 1996, *AJ*, 112, 2639
- Shetrone, M. d. 2003, *ApJ*, 585, 45
- Schlegel, D. J., Finkbeiner, D. P., & Davis, M. 1998, *ApJ*, 500, 525
- Smith V. V., Terndrup, D. M., & Suntzeff, N. B. 2002, *ApJ*, 579, 832
- Sneden, C., Kraft, R. P., Guhathakurta, P., Peterson, R. C., Fulbright, J. P. 2004, *AJ*, 127, 2162
- Suntzeff, N. B., & Smith, V. V. 1991, *ApJ*, 381, 160
- Valenti, E., Ferraro, F.R., & Origlia, L. 2004, *MNRAS*, 351, 1204
- Vanture, A. D., Wallerstein, G., & Suntzeff, N. B. 2002, *ApJ*, 569, 984
- Ventura, P., D'Antona, F., Mazzitelli, I., & Gratton, R. 2001, *ApJ*, 550, 65